Life Sciences 231 (2019) 116558

Contents lists available at ScienceDirect

Life Sciences

journal homepage: www.elsevier.com/locate/lifescie

SIRT6 as a potential target for treating insulin resistance

Wei Tang*, Yingying Fan

Department of Endocrinology, Zhoukou Central Hospital, Zhoukou, Henan, China

ARTICLE INFO

Keywords:
Insulin resistance
High-fat diet-fed obese mouse
SIRT6
TRPV1

ABSTRACT

Aims: We aimed to explore the role of SIRT6 in Insulin resistance (IR). We are the first to investigate on this crucial relationship in an obese mouse model fed on a high-fat diet (HFD) and an IR model based on the mature 3T3-L1-derived adipocytes.

Main methods: Western blotting (WB) and qPCR analysis were performed to evaluate the SIRT6 protein and mRNA expressions in HFD mice as well as IR cells. Injection of adenovirus encoding SIRT6 gene in HFD mice and transfection of pcDNA3-SIRT6 in IR cells increased the glucose uptake levels and insulin sensitivity.

Key findings: The positive regulatory effects of SIRT6 on transient receptor potential vallinoid 1 (TRPV1) in IR cells were confirmed by a mechanistic investigation at both protein and mRNA levels. Further, the overexpression of SIRT6 was found to activate the TRPV1/Calcitonin gene-related peptide (CGRP) signaling and upregulate the glucose transporter (GLUT) expression at protein and mRNA levels. Additionally, administration of the TRPV1 antagonist, SB-705498 repressed the insulin sensitivity upregulated by SIRT6 overexpression accompanied with the inhibition of CGRP and decrease in GLUT proportions. The results also showed that TRPV1 agonist, Capsaicin boosted the SIRT6-induced glucose uptake, CGRP production, and GLUT4 levels.

Significance: Overall, SIRT6 was concluded to be involved in the TRPV1-CGRP-GLUT4 signaling axis thus leading to increased glucose uptake and decreased IR in HFD mice and 3T3-L1 adipocytes. Therefore, in terms of obesity and diabetes, SIRT6 is a novel candidate for treating IR.

1. Introduction

Type 2 diabetes (T2D) has been recognized as a global prominent health issue that affects children as well as adults [1,2]. Over the past 30 years, the occurrence of T2D has been prevalently rising and thus, an in-depth understanding of its complex pathologic mechanism needs to be achieved. The major pathogenic factors of T2D reported are genetic, obesity, lifestyle, and impaired glucose tolerance [3,4]. Insulin resistance (IR) is a major leading cause for impaired glucose metabolism, which is a critical component of metabolic syndrome [5]. IR is considered an attenuated capability of targeted cells such as adipocytes, hepatocytes, and skeletal muscle cells in the presence of insulin [6]. IR induces impairment in the synthesis of glycogen and promotes unregulated production of glucose in the liver. However, the molecular mechanism responsible for IR in hepatocytes is still not known.

Sirtuins have been recognized as deacetylases that are dependent on NAD+ and have mediating roles in a variety of biological processes, thereby playing a part in the progression of many different diseases. SIRT6 belongs to a family of sirtuins that was first generated by cloning from the cDNA library of the human spleen [7]. SIRT6 has inhibitory effects on the transcription of its target genes by deacetylating histone H3 at specific sites [8,9]. Besides, SIRT6 has controlling or mediating effects on inflammatory responses, maintenance of chromosome integrity, and many other biological functions [8,9]. Increased evidence suggests that reduction in the SIRT6 activity induced by factors such as overnutrition and aging is associated with obesity and diabetes. This can lead to abnormality in lipid and glucose metabolism. Serious hypoglycemic syndrome has been reported in the mouse model after SIRT6 knockout [10–13]. Studies also show that steatosis of liver can be aggravated after ablating SIRT6 in a hepatic-specific manner [14]. The blood glucose levels were found to be increased after deleting SIRT6 in a fat-specific way wherein the steatosis of liver was also aggravated. In this case, the IR and obesity that were induced by diet were also increased in the absence of SIRT6 [12,13,15]. In another study, the IR and obesity induced by diet were also increased after neural-specific SIRT6 deletion in the mouse model [16]. The diet-induced IR and obesity were potentially avoided on the overexpression of SIRT6 [11]. However, its role and molecular mechanism in a high-fat diet (HFD) mouse and IR cells has not been completely elucidated.

To further characterize the underlying mechanism of SIRT6-mediated HFD mice and IR adipocytes, the present study established an obese mouse model (based on HFD mice) as well as a TNF-α-induced IR

* Corresponding author at: Department of Endocrinology, Zhoukou Central Hospital, No. 26, Renmin Road, Zhoukou, Henan 466000, China.
E-mail address: tangweinar@163.com (W. Tang).

https://doi.org/10.1016/j.lfs.2019.116558
Received 23 April 2019; Received in revised form 4 June 2019; Accepted 10 June 2019
Available online 11 June 2019
0024-3205/

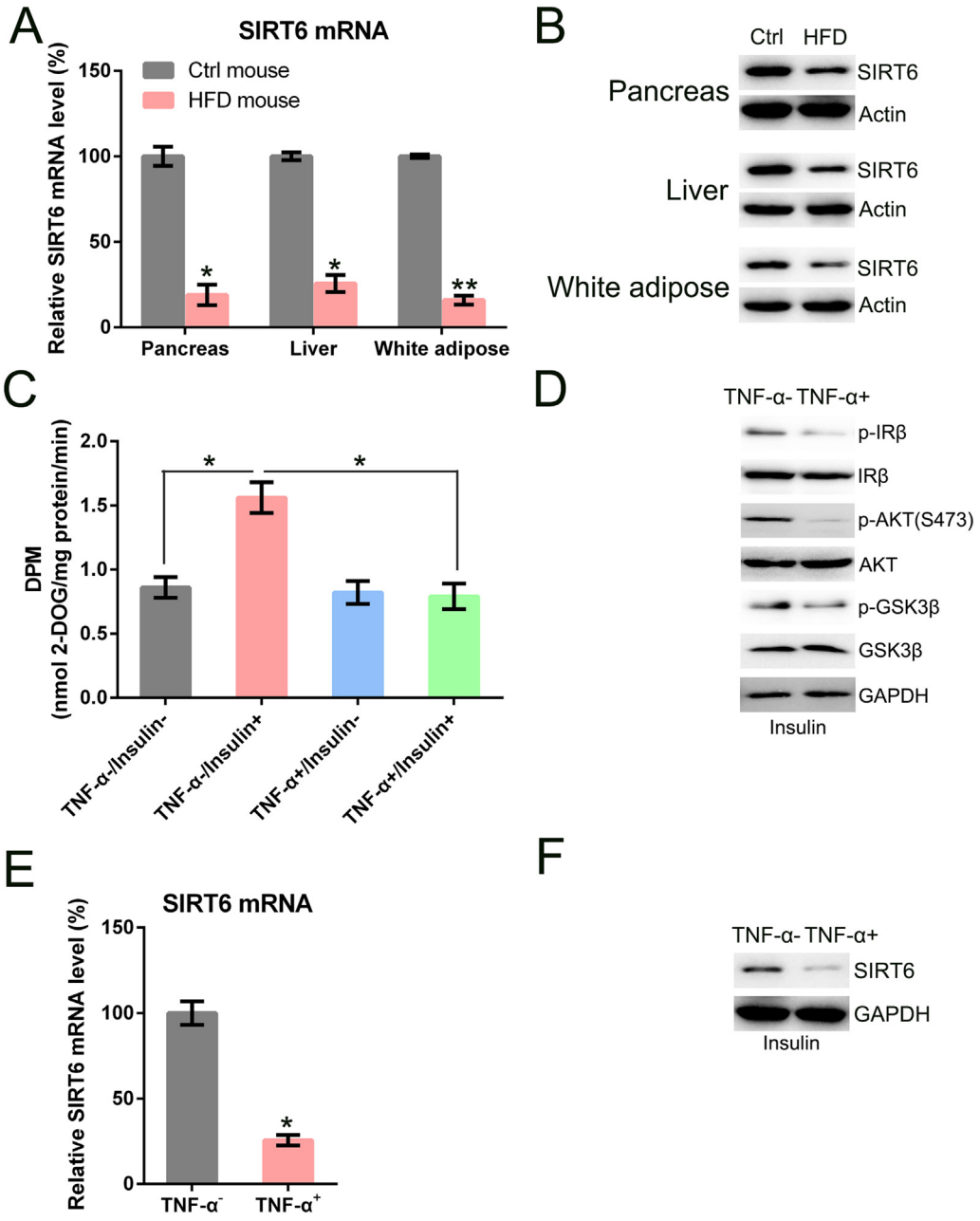

Fig. 1. Down-regulation of SIRT6 in HFD-fed mice and IR cells.
(A, B) For HFD-obese mice, a decrease in the expression of SIRT6 was observed in the liver, pancreas, and white adipose tissues using real-time PCR and WB analysis at week 10. (C) Cells were treated with high-glucose DMEM that contained FBS (10%, w/v) supplemented with TNF-α (10 ng/mL) for 24 h. Subsequently, they were incubated for 0.5 h with another cell medium comprising insulin (100 nM) in high-glucose DMEM containing FBS (10%, w/v). The establishment of the IR adipocyte model was confirmed by 2-DOG assay. (D) WB analysis was performed to detect the expression of IRβ, AKT, and GSK3β after TNF-α treatment (E, F) qPCR and WB were utilized showing a sharp down-regulation of SIRT6 expression in IR cell model treated with TNF-α compared to the expression in the normal control 3T3-L1 cells. $^{*}P < 0.05$, $^{**}P < 0.01$, on comparing with the indicated groups were considered significant.

adipocyte cell model to elucidate the role of SIRT6 in IR and glucose metabolism. Our results showed that TRPV1 served as a target for SIRT6 regulation in controlling IR and glucose metabolism. Therefore, this study confirmed that SIRT6 is a promising candidate to treat IR in obesity and T2D.

2. Materials and methods

2.1. Animal and treatment

C57BL/6 male mice ($n = 24$) were commercially bought from Vital River Laboratories (Beijing, China). A diet-induced obesity model was established as previously reported [17]. Briefly, HFD was provided to the 4-week old mice ($n = 6$) (Research Diet, USA; 45% kcal fat), or with standard chow diet (n = 6) for a period of 10 weeks. The experiments were performed under controlled humidity and temperature conditions (45–55% and 20–24 °C, respectively).

The mice were intravenously injected *via* tail vein with adenovirus-encoding green fluorescent protein (Ad-NC, $n = 6$) or SIRT6 (Ad-SIRT6, n = 6) at a dosage of 1 × 108 PFU in 0.2 mL PBS (0.2 mL/25 g body weight). On the 9th day post injection, mice were sacrificed and tissues such as the pancreas, liver, and white adipose were collected. The tissues were assayed by real-time quantitative PCR (rtPCR) along with western blotting (WB). The experiments in this mouse study were performed with the suggestions and approval from National Research Council Guide for Care and Use of Laboratory Animals under the protocol of Animal Ethics Committee of Zhoukou Central Hospital.

2.2. Cell cultivation and transfection

The mouse 3T3-L1 cell line used in this study was obtained from the Shanghai Institutes for Biological Sciences, Chinese Academy of Sciences. At first, RPMI-1640 media with 100 U/mL penicillin, 100 mg/mL streptomycin (Gibco), 10% fetal bovine serum (FBS, Gibco), and 2 mmol/L glutamine was prepared for the cultivation of 3T3-L1 preadipocytes. Following cultivation, the preadipocytes were incubated in

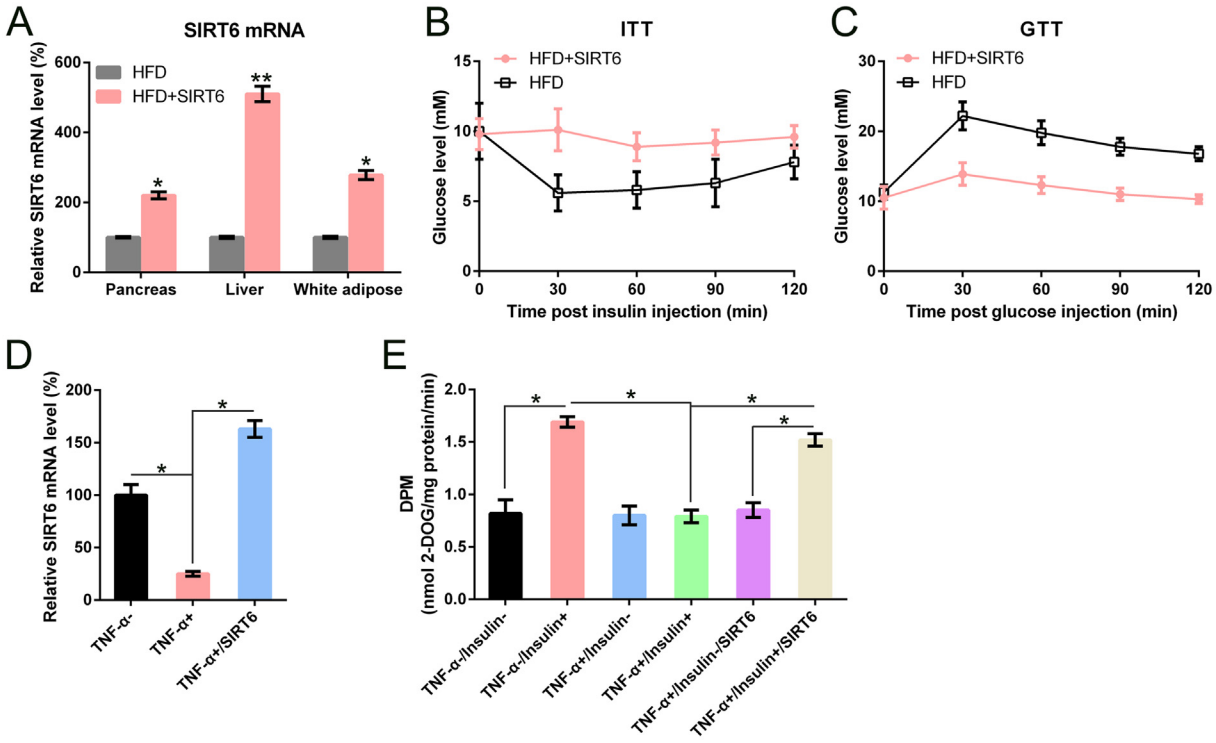

Fig. 2. SIRT6 overexpression-induced hyperglycemia amelioration and IR prevention in obese mouse model and IR cells.
C57BL/6 mice were induced with 10-week HFD (Research Diet, USA; 45% kcal fat) or with 10-week standard chow diet. The mice were treated with intravenous injection of Ad-ctrl and Ad-SIRT6. (A) Expression of SIRT6 was determined in the liver, pancreas, and white adipose tissues using qPCR. (B) Glucose tolerance test (GTT) was performed in the HFD-obese mice at day 7 post Ad-ctrl or Ad-SIRT6 injection. (C) Insulin tolerance test (ITT) was performed in the HFD- obese mice at day 7 post Ad-ctrl or Ad-SIRT6 injection. (D) In the IR 3T3-L1 cells transfected with pcDNA3-SIRT6 or pcDNA3 vector, the SIRT6 expression levels were studied by qPCR. (E) Glucose uptake levels were tested in IR 3T3-L1 cells transfected with SIRT6 vector by 2-deoxyglucose uptake assay (2-DOG). $^{*}P < 0.05$, $^{**}P < 0.01$, on comparing with the indicated groups were considered significant.

CO_2 (5%) at 37 °C. The cells were induced for differentiation into adipocytes according to the protocol described in the previous literature [18,19]. In brief, a differentiation mixture that contained 10 μg/mL insulin, 1 μM dexamethasone, and 0.5 mM 3-isobutyl-1-methylxanthine in DMEM with 10% FBS was prepared and used for the differentiation of the 3T3-L1 preadipocytes (on 100% confluency) for 48 h. Cells were then cultivated for 10 days in 10% FBS-DMEM supplemented with insulin (10 μg/mL). Finally, the mature adipocytes were confirmed using light microscopy with oil red O staining before using in subsequent experiments.

2.3. IR adipocyte model establishment

It has been widely reported that the resistance to insulin is partly caused by tumor necrosis factor-α (TNF-α) and plays a key role in the pathogenesis of type 2 diabetes and obesity [20–22]. At first, the differentiated 3T3-L1 adipocytes were cultured in high-glucose DMEM containing FBS (0.5%, w/v) for 3 h as a pretreatment. Further treatment was conducted using high-glucose DMEM containing FBS (10%, w/v) supplemented with TNF-α (10 ng/mL) for 24 h. Subsequently, the cells were incubated for 0.5 h with a different cell medium comprising of insulin (100 nM) in high-glucose DMEM containing FBS (10%, w/v). To verify the successful construction of an insulin-resistant cell model, the glucose assay kit (Sigma-Aldrich, USA) was employed for the detection of glucose.

2.4. Recombinant adenovirus preparation

Based on the previous literature, recombinant adenoviruses that expressed a SIRT6 or a negative control (Ctrl) adenovirus vector were made commercially available from Shanghai GeneChem Co., Ltd. (China) [23].

Glucose- and insulin-tolerance tests (GTT and ITT).

After 12 h of fasting, the mice were injected intraperitoneally using 2 g/kg D-glucose. During the insulin tolerance test (ITT assay) before injection, the concentration of the recombinant human insulin was adjusted from 100 U/mL to 0.075 U/mL through dilution in saline. At 12 h after food deprivation, the mice were treated with intraperitoneal insulin injection (0.1 mL/10 g body weight). At 15, 30, 45, 60, and 90 min, the blood glucose levels were measured with a glucometer (One Touch Ultra) using the blood samples collected from the mice tail vein.

2.5. 2-Deoxyglucose (2-DOG) uptake measurement

An improved protocol as described in previous literature was used for the glucose uptake tests. Briefly, Krebs-Ringer phosphate buffer was used for washing (3 times) the pre-treated cells, followed by a 10 min cell incubation in a final concentration of 1 μCi/mL ^{3}H-2-DG (GE healthcare, USA). Krebs-Ringer phosphate buffer was then used for terminating the reaction. Cells were lysed using NaOH (0.1 N) and a scintillation counter (LS 6500, Beckman, USA) was used for the measurement of radioactivity (DPM). Eventually, DPM correction was conducted for the content of protein assayed by BCA protein measurement in each well.

2.6. Western blot

Cell lysis was performed with a protease suppressor cocktail (Roche, Switzerland) in a RIPA buffer (pH 8.0) containing 1% NP-40, 0.1% SDS, 50 mM Tris-HCl, and 150 mM NaCl. A BCA Protein Quantitation Kit was employed for the quantification of proteins. On a 10% SDS-PAGE gel, the protein samples were isolated and transferred onto a 0.45 μm PVDF

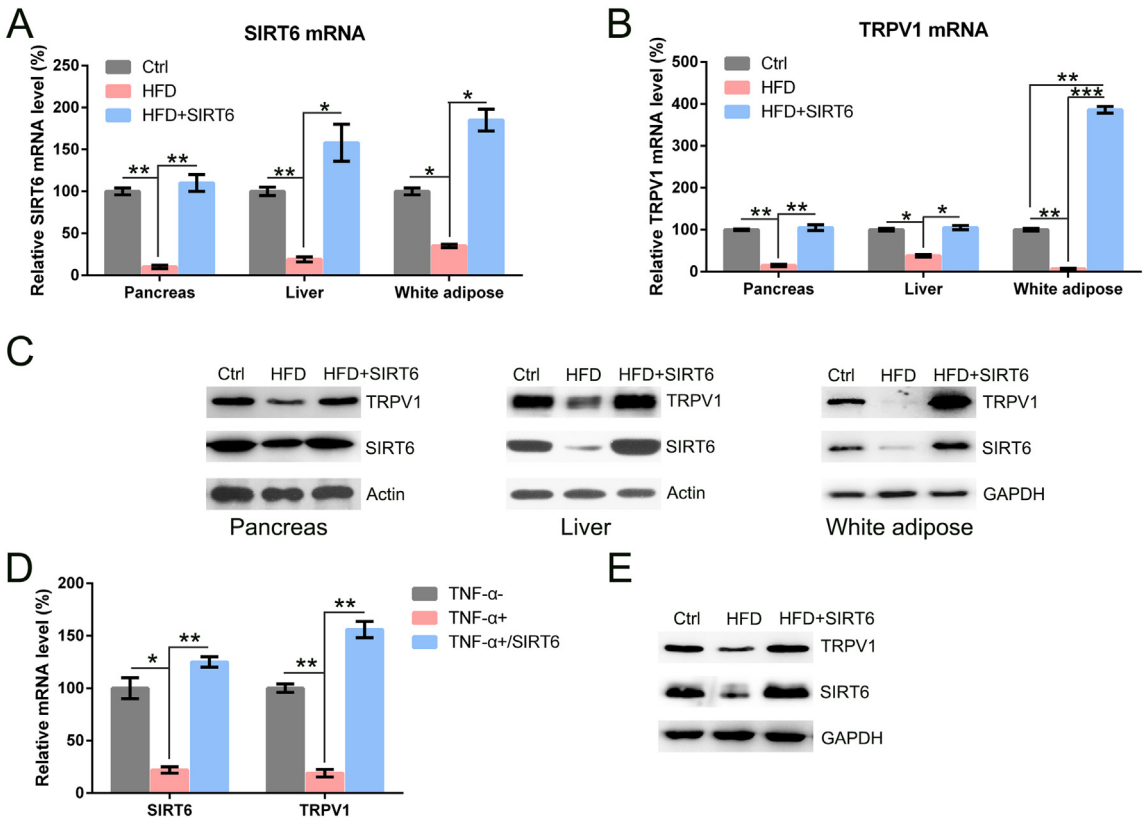

Fig. 3. SIRT6 positively regulated the expression of TRPV1 channel.
C57BL/6 mice were induced with 10-week HFD (Research Diet, USA; 45% kcal fat) or with 10-week standard chow diet. The mice were treated with intravenous injection of Ad-ctrl and Ad-SIRT6. Expressions of (A) SIRT6 and (B) TRPV1 were determined in the liver, pancreas, and white adipose tissues using qPCR, and (C) WB. qPCR (D) and WB assay (E) showed that SIRT6 upregulation significantly increased the expression of TRPV1 protein as well as mRNA levels. *$P < 0.05$, **$P < 0.01$, ***$P < 0.001$, on comparing with the indicated groups were considered significant.

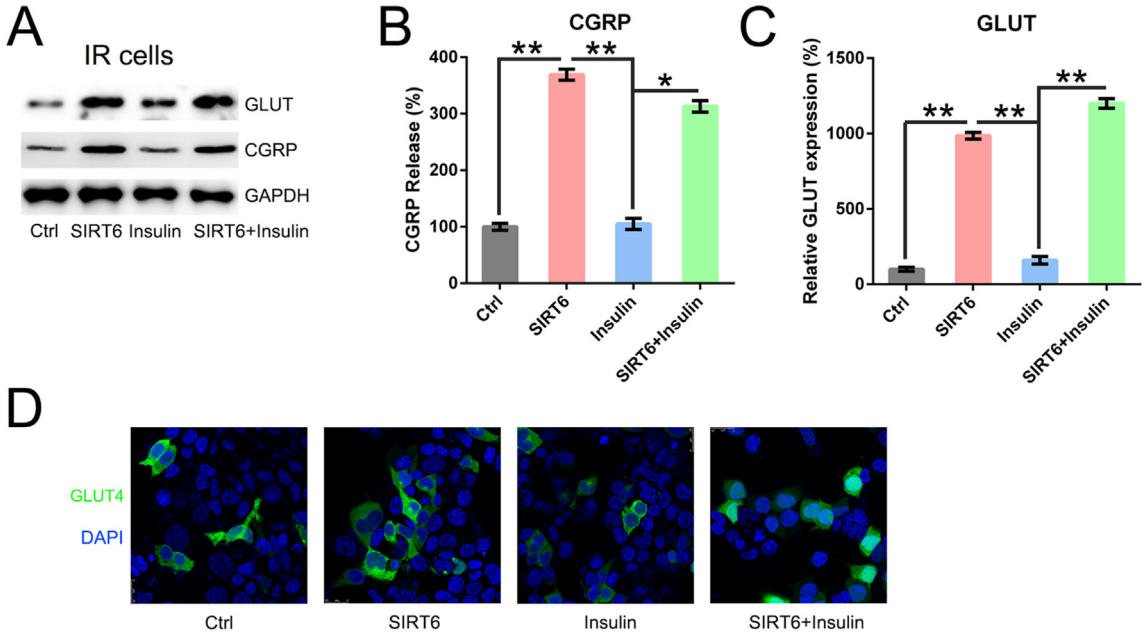

Fig. 4. Roles of SIRT6 in the TRPV1 activation and GLUT expression in IR 3T3-L1 cells.
SIRT6 or control vector was used for cell transfection, followed by treatment with 10 ng/mL TNF-α and/or 100 nM insulin in high-glucose DMEM containing FBS (10%, w/v). (A) WB displayed that SIRT6 vector transfection led to GLUT upregulation and CGRP expression. (B) The released CGRP levels in cells were measured by ELISA under different treatment conditions. (C) GLUT mRNA expression was detected by qPCR test in IR 3T3-L1 cells under different treatment conditions. (D) Immunofluorescence analysis (IFA) showed that GLUT4 staining was increased and transported to nucleus after SIRT6 transfection. *P < 0.05, **P < 0.01, on comparing with the indicated groups were considered significant.

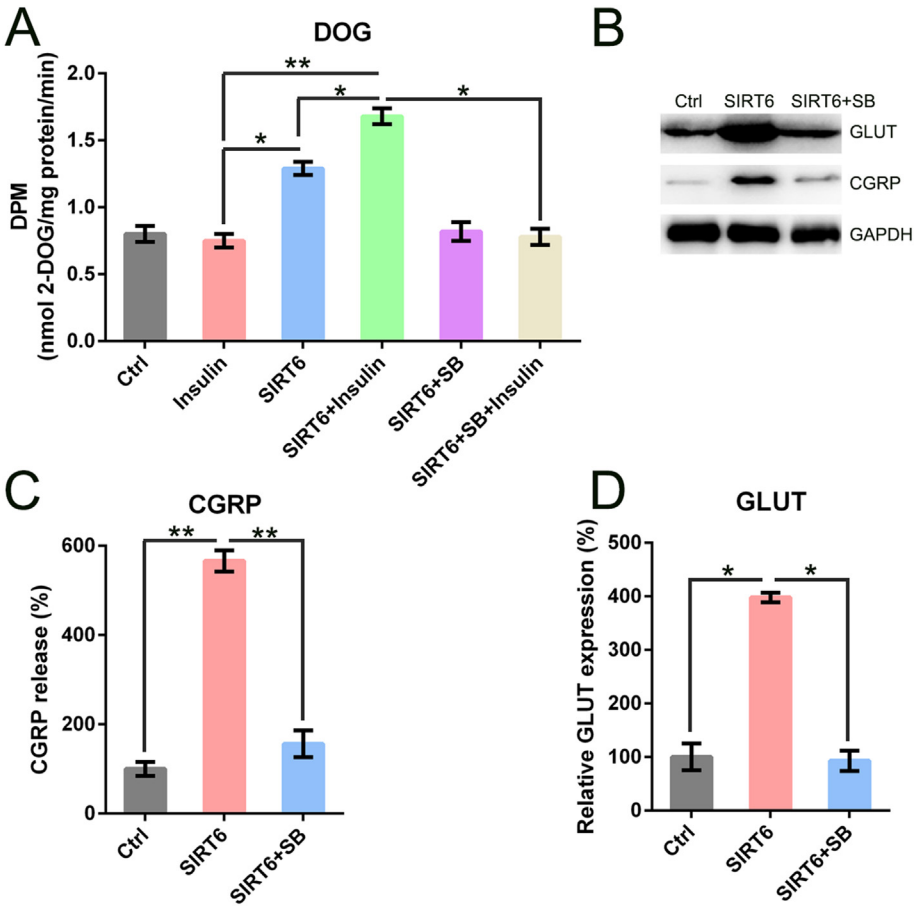

Fig. 5. TRPV1 inhibitor SB-705498 reversed the effect of SIRT6 overexpression on insulin sensitivity. (A) The effect of TRPV1 inhibitor, SB-705498 (SB, 1 μM) on insulin sensitivity was assessed by studying the glucose uptake level in IR 3T3-L1 cells under different treatment conditions. (B) The expression of CGRP and GLUT in cells with or without SB (1 μM) treatment for 24 h was determined by WB assay. (C) The released CGRP levels in cells under different treatment conditions were determined by ELISA. (D) qPCR results showed that the GLUT expression was inhibited by SB treatment. *P < 0.05, **P < 0.01, on comparing with the indicated groups were considered significant.

membrane. The membranes were blocked for 1 h with PBST containing BSA (5%) at ambient temperature, followed by primary antibody incubation using specific antibodies: anti-actin, anti-Bax, anti-Bcl-2, and anti-SIRT6 at 4 °C for 60 min. Then, the membranes were incubated using secondary antibodies that were conjugated to Amersham ECL peroxidase: goat anti-rabbit immunoglobulin G (1:10,000) or goat anti-mouse immunoglobulin G (1:10,000) at ambient temperature for 1 h. The immunoreactivity was measured with a SuperSignal West Femto Maximum Sensitivity Substrate Kit (Thermofisher scientific, USA) on a C-DiGit Blot Scanner.

2.7. RNA extraction and qPCR

Trizol reagent was used to isolate total RNA from the 3T3-L1 cells. Transcription levels were analyzed with the Roche Light-Cycler 480 Real Time PCR system with GAPDH as the internal reference control. SYBR Green PCR Master Mix was used for qPCR (20 μL). PCR cycling was performed as below: initial denaturation at 95 °C for 10 min, 40 cycles of denaturation at 95 °C for 15 s, annealing at 60 °C for 0.5 min, and extension at 72 °C for 0.5 min. Quantification was performed according to the 2-ΔΔCT method through normalization to GAPDH with reference to the calibrator (mean of the control samples).

2.8. ELISA measurement

In cell supernatants, the calcitonin gene-related peptide (CGRP) levels were measured using ELISA kit (R&D Systems, Minneapolis, MN, USA) as per manufacturer's instructions. For comparative analysis, the absorbance was recorded using microplate reader (BMG Labtech, Offenburg, Germany; OD: 543 nm).

Immunofluorescence assays (IFA).

Cell transfection was carried out using the 3T3-L1 cells. The cells were grown in 24-well plates with cover slides. Cells were then fixed at ambient temperature for 60 min using 4% paraformaldehyde in PBS. This was followed by 10-min cell permeabilization at 25 °C using PBST. Cells were then blocked in PBST containing 0.4% BSA at 37 °C for 60 min followed by polyclonal anti-GLUT antibody (diluted in PBST containing 0.2% BSA) primary antibody incubation for another 60 min at 37 °C. The cells were washed with PBST for 60 min. TRITC-labeled goat anti-rabbit antibody (diluted in 0.2% BSA /PBST) as secondary antibody was used at 37 °C for 60 min followed by 60 min of PBST washing. Cell nuclei were stained using DAPI. The VP1 staining in cells was analyzed using FITC filter of a confocal laser scanning fluorescence microscope (Olympus LSCMFV500, Japan).

2.9. Data analysis

Data are represented as mean ± standard deviation (SD) values. The intergroup difference was analyzed using the one-way analysis of variance or two-tailed Student's *t*-test where statistical significance was considered at $P < 0.05$.

3. Results

3.1. Downregulation of SIRT6 levels in obese mice models and IR cells

An HFD-induced obese mice model and IR 3T3-L1 cell model were established to study the role of SIRT6 in glucose metabolism and insulin resistance. At First, SIRT6 expressions at the mRNA and protein level in the pancreatic tissues of obese mice showed sharp downregulation compared to the control group (Fig. 1A and B). For *in vitro* study, IR cells were obtained by pre-incubation with TNF-α in 3T3-L1-induced

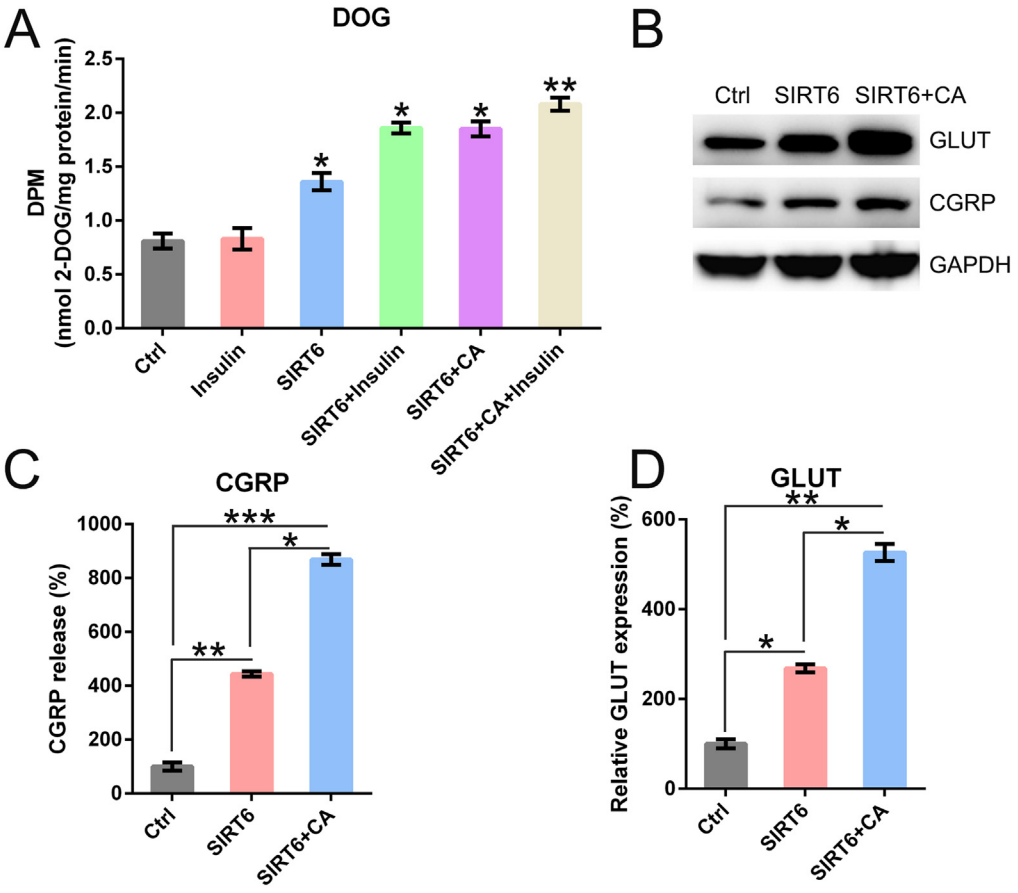

Fig. 6. TRPV1 agonist capsaicin amplified the effect of SIRT6 overexpression on insulin sensitive cells.
In the IR 3T3-L1 cells, glucose uptake level was examined under different treatment conditions to assess the effects of TRPV1 inhibitor, capsaicin (CA, 3 μM) on insulin sensitivity. (B) With or without CA treatment (3 μM) for 24 h, the expressions of GLUT and CGRP in cells were detected by WB assay. (C) Under different treatment conditions, the released CGRP levels in cells were detected by ELISA. (D) qPCR results showed that GLUT expression was inhibited by CA treatment. *P < 0.05, **P < 0.01, on comparing with the indicated groups were considered significant.

adipocytes and confirmed with respect to the glucose uptake detection capability by 2-DOG assay in the presence and absence of insulin. In the absence of TNF-α, the glucose uptake levels were raised after adding insulin in the 3T3-L1-induced adipocytes (Fig. 1C). However, no variation was observed for the glucose uptake levels after TNF-α pre-incubation with or without insulin treatment. Lower glucose uptake levels suggested that a successful IR model in adipocytes was established. To further confirm the IR modeling, we determined the expression and phosphorylation of Insulin Receptor beta subunit (IRβ), AKT, and GSK3β after TNF-α treatment. Our data indicated that TNF-α damaged the insulin signaling (Fig. 1D). Similar to the mouse model, qPCR and WB data showed that SIRT6 also decreased after TNF-α pre-incubation in IR cells (Fig. 1E and F).

3.2. Regulation of glucose metabolism and IR in HFD-fed mice and IR 3T3-L1 cell by SIRT6 overexpression

To study the role of SIRT6 in IR and glucose metabolism in *in vivo* animal and *in vitro* cell models, the mice fed with HFD were intravenously injected with the recombinant adenovirus expressing SIRT6 (Ad-SIRT6) or a control (Ad-ctrl) through the tail vein. Injection of Ad-SIRT6 increased SIRT6 mRNA expression level in the pancreas, liver, and white adipose tissues (Fig. 2A). In the presence of insulin, the trend in blood glucose level reduction intensified as shown in Fig. 2B. Thus, it was observed that in the obese mice, the insulin sensitivity was enhanced after SIRT6 overexpression. Compared to the mice treated with Ad-ctrl, the Ad-SIRT6-injected mice fed with HFD showed severe decrease in the fasting blood glucose levels. The oral glucose tolerance experiment results indicated that the reduction in SIRT6 level could evidently elevate the glucose tolerance, as shown in Fig. 2C.

IR 3T3-L1 cells were also transfected with SIRT6-expressing vector. For each group, the qPCR assay was conducted to measure the SIRT6 expression level (Fig. 2D). The glucose uptake levels in cells displayed a remarkable upregulation under SIRT6 overexpression in the IR 3T3-L1 adipocytes when compared to the control group (Fig. 2E). Thus, the data suggested that SIRT6 plays a key role in increasing insulin sensitivity.

3.3. SIRT6 regulates TRPV1 expression

The expression level of TRPV1 was studied in obese mice and IR cells by qPCR and WB. It has been reported that TRPV1 is regulated by SIRT6 [24], and it plays an essential role in IR and glucose metabolism [25]. Our results in the obese mice and IR cells exhibited similar trend of abated TRPV1 expression whereas its expression was restored following with SIRT6 overexpression by injection of Ad-SIRT6 (Fig. 3A–C). WB and qPCR assays were performed to study the role of SIRT6 in TRPV1 expression in IR 3T3-L1 cells. Further, TRPV1 synthesis was investigated by transfecting IR 3T3-L1 adipocytes using a SIRT6-expressing vector or control vector. The results showed that SIRT6 expression was augmented after SIRT6 transfection (Fig. 3D and E) which suggested that SIRT6 positively regulates TRPV1 expression.

3.4. Expression of SIRT6 is related to GLUT expression and CGRP production in IR cells

As it has already been reported that TRPV1 is a transporter of CGRP and regulator of GLUT expression [25], we determined the CGRP and GLUT expression levels, and CGRP release in IR cells after transfection with SIRT6-expressing vector. Upregulation of CGRP expression was confirmed by WB (Fig. 4A) and CGRP release was also intensified (Fig. 4B). WB, qPCR, and IFA showed that GLUT4 levels were also increased in SIRT6-overexpressing cells, and GLUT4 transported to nucleus after SIRT6 transfection (Fig. 4A, C and D). Thus, it was evident

that SIRT6 is positively associated with CGRP and GLUT4 levels.

3.5. TRPV1 is responsible for the SIRT6-mediated insulin sensitivity

To confirm the effects of TPRV1 on SIRT6-regulated insulin sensitivity, TPRV1 inhibitor, SB-705498 was added to the medium of SIRT6-transfected IR cells. The results showed that SB-705498 treatment reversed the glucose uptake that had been increased by SIRT6 overexpression (Fig. 5A). Furthermore, GLUT expression was rapidly reduced with the SB-705498 treatment (Fig. 5B and D) while CGRP expression and release were also blocked (Fig. 5B and C).

The effects of TRPV1/CGRP signaling on the insulin sensitivity that was regulated by SIRT6 were further studied by treating the SIRT6-transfected IR cells by a TRPV1 agonist, capsaicin. The results showed that the increased glucose uptake level was further amplified after capsaicin treatment (Fig. 6A). Additionally, CGRP expression and release in SIRT6 + capsaicin group was higher than that in the SIRT6-only group (Fig. 6B and C) while GLUT mRNA and protein expression levels were significantly improved (Fig. 6B and D).

4. Discussion

The present work revealed a reduction in SIRT6 expression in obese mouse and IR cell model and increase in glucose uptake levels and insulin sensitivity in case of SIRT6 overexpression. Further investigation revealed that SIRT6 overexpression promotes TRPV1 expression levels. Overexpression of SIRT6 was found to promote the activation of TRPV1/CGRP signaling and GLUT expression at mRNA as well as protein levels. Usage of TRPV1 agonist and antagonist modified the insulin sensitivity upregulated by SIRT6 overexpression and accompanied with the mediation of CGRP release and decrease in GLUT levels. The results of this study revealed that SIRT6 had a suppressing role in IR mice and cells by regulating the expression of TRPV1 protein. Therefore, we hypothesize that SIRT6 can be a potential candidate to treat IR in metabolic syndrome.

Several methods were explored to establish an IR model at the cellular level, such as dexamethasone in FL83B cells [26], pretreatment with dexamethasone in L6 myotubes [26], and HepG2 cells induced by palmitate and glucosamine [27]. However, in this study, we established the IR model in 3T3-L1 adipocytes using TNF-α. Furthermore, a lower glucose uptake level determined by glucose detection assay (2-DOG) suggested the successful establishment of an IR cell model. For animal model, obese mice were treated with HFD. HFD leads to skeletal muscle IR by upregulating free fatty acids, which produces diacylglycerols (DAGs) and ceramides as intermediate metabolites. The DAGs activate serine/threonine kinases by activating protein kinase C family and phosphorylate IRS tyrosine. In turn, the ceramides can lead to Akt2 phosphorylation by activating protein phosphatase A2. Additionally, ceramides also induce IR by activating the NF-kappa-b, JNK, and other inflammatory pathways [28].

The expression of TRP protein super-family as cation-permeable channels has already been reported in mammalian cells. TRPV1 channel is a perfect representative. TRPV1, characterized by nonselectivity, is involved in pain sensation and thermogenesis and shows high Na^+ and Ca^{2+} permeation [29-31]. As a main constituent of the plant family *Capsicum* (chili pepper), capsaicin causes spicy sensation including thermogenic responses and pain as a specific and natural TRPV1 channel agonist [25], whereas a selective and powerful antagonist for TRPV1 receptor, SB-705498, was found to have an inhibitory effect on the receptor activation, which was mediated by heat, acid, and capsaicin [32]. TRPV1 channel could cause neurogenic inflammation *via* the CRTC1/cAMP response element binding (CREB) signaling to upregulate CGRP expression [33]. SB-705498 and capsaicin cause nerve injury *via* spontaneous inflammation by down- and up-regulating the activity of TRPV1, respectively [34,35]. In the present study, IR model reduced the TRPV1 expression and activity, which was accompanied by SIRT6 downregulation. Our data also showed that elevated CGRP release and expression levels were found in HFD-fed mice and TNF-α-treated cells. However, the CGRP release was suppressed on SIRT6 overexpression. In this work, SB-705498 and capsaicin were utilized to confirm the role of TRPV1/CGRP pathway in IR and glucose metabolism followed by detection of glucose uptake and GLUT expression. The results indicated that dysregulation in IR and glucose metabolism stimulated by HFD and TNF-α was significantly inhibited on SIRT6 overexpression.

5. Conclusion

Collectively, our data prove the absence of SIRT6 in human HFD-fed mice and IR cell model, and repression of IR and increased glucose metabolism can be caused by SIRT6 overexpression. Thus, we hypothesize that SIRT6-TRPV1-CGRP may be a crucial axis in regulating the insulin resistance and glucose uptake; thus, SIRT6 is a suitable candidate for treating IR as well as obesity.

Authors' contributions

In this work, TW and FYY conceived the study and designed the experiments; contributed to the data collection; performed the data analysis and interpreted the results. TW wrote the manuscript; TW and FYY contributed to the critical revision of article. Both authors read and approved the final manuscript.

Research involving human participants and/or animals

All applicable international, national, and/or institutional guidelines for the care and use of animals were followed.

Funding

None.

Declaration of Competing Interest

The authors declare that they have no competing interests.

Acknowledgments

None.

References

[1] M. Abu-Farha, J. Abubaker, I. Al-Khairi, P. Cherian, F. Noronha, F.B. Hu, K. Behbehani, N. Elkum, Higher plasma betatrophin/ANGPTL8 level in type 2 diabetes subjects does not correlate with blood glucose or insulin resistance, Sci. Rep. 5 (2015) 10949.
[2] S. Tangvarasittichai, Oxidative stress, insulin resistance, dyslipidemia and type 2 diabetes mellitus, World J. Diabetes 6 (2015) 456–480.
[3] C.J. Nolan, N.B. Ruderman, S.E. Kahn, O. Pedersen, M. Prentki, Insulin resistance as a physiological defense against metabolic stress: implications for the management of subsets of type 2 diabetes, Diabetes 64 (2015) 673–686.
[4] C. Chakraborty, C.G. Doss, S. Bandyopadhyay, G. Agoramoorthy, Influence of miRNA in insulin signaling pathway and insulin resistance: micro-molecules with a major role in type-2 diabetes, Wiley Interdiscip. Rev. RNA 5 (2014) 697–712.
[5] E. Ferrannini, B. Balkau, S.W. Coppack, J.M. Dekker, A. Mari, J. Nolan, M. Walker, A. Natali, H. Beck-Nielsen, R. Investigators, Insulin resistance, insulin response, and obesity as indicators of metabolic risk, J. Clin. Endocrinol. Metab. 92 (2007) 2885–2892.
[6] K. Avall, Y. Ali, I.B. Leibiger, B. Leibiger, T. Moede, M. Paschen, A. Dicker, E. Dare, M. Kohler, E. Ilegems, M.H. Abdulreda, M. Graham, R.M. Crooke, V.S. Tay, E. Refai, S.K. Nilsson, S. Jacob, L. Selander, P.O. Berggren, L. Juntti-Berggren, Apolipoprotein CIII links islet insulin resistance to beta-cell failure in diabetes, Proc. Natl. Acad. Sci. U. S. A. 112 (2015) E2611–E2619.
[7] G. Liszt, E. Ford, M. Kurtev, L. Guarente, Mouse Sir2 homolog SIRT6 is a nuclear ADP-ribosyltransferase, J. Biol. Chem. 280 (2005) 21313–21320.
[8] L. Zhong, A. D'Urso, D. Toiber, C. Sebastian, R.E. Henry, D.D. Vadysirisack, A. Guimaraes, B. Marinelli, J.D. Wikstrom, T. Nir, C.B. Clish, B. Vaitheesvaran,

O. Iliopoulos, I. Kurland, Y. Dor, R. Weissleder, O.S. Shirihai, L.W. Ellisen, J.M. Espinosa, R. Mostoslavsky, The histone deacetylase Sirt6 regulates glucose homeostasis via Hif1alpha, Cell 140 (2010) 280–293.
[9] D. Toiber, F. Erdel, K. Bouazoune, D.M. Silberman, L. Zhong, P. Mulligan, C. Sebastian, C. Cosentino, B. Martinez-Pastor, S. Giacosa, A. D'Urso, A.M. Naar, R. Kingston, K. Rippe, R. Mostoslavsky, SIRT6 recruits SNF2H to DNA break sites, preventing genomic instability through chromatin remodeling, Mol. Cell 51 (2013) 454–468.
[10] Y. Kanfi, R. Shalman, V. Peshti, S.N. Pilosof, Y.M. Gozlan, K.J. Pearson, B. Lerrer, D. Moazed, J.C. Marine, R. de Cabo, H.Y. Cohen, Regulation of SIRT6 protein levels by nutrient availability, FEBS Lett. 582 (2008) 543–548.
[11] Y. Kanfi, V. Peshti, R. Gil, S. Naiman, L. Nahum, E. Levin, N. Kronfeld-Schor, H.Y. Cohen, SIRT6 protects against pathological damage caused by diet-induced obesity, Aging Cell 9 (2010) 162–173.
[12] J. Kuang, Y. Zhang, Q. Liu, J. Shen, S. Pu, S. Cheng, L. Chen, H. Li, T. Wu, R. Li, Y. Li, M. Zou, Z. Zhang, W. Jiang, G. Xu, A. Qu, W. Xie, J. He, Fat-specific Sirt6 ablation sensitizes mice to high-fat diet-induced obesity and insulin resistance by inhibiting lipolysis, Diabetes 66 (2017) 1159–1171.
[13] L. Yao, X. Cui, Q. Chen, X. Yang, F. Fang, J. Zhang, G. Liu, W. Jin, Y. Chang, Cold-inducible SIRT6 regulates thermogenesis of brown and beige fat, Cell Rep. 20 (2017) 641–654.
[14] H.S. Kim, C. Xiao, R.H. Wang, T. Lahusen, X. Xu, A. Vassilopoulos, G. Vazquez-Ortiz, W.I. Jeong, O. Park, S.H. Ki, B. Gao, C.X. Deng, Hepatic-specific disruption of SIRT6 in mice results in fatty liver formation due to enhanced glycolysis and triglyceride synthesis, Cell Metab. 12 (2010) 224–236.
[15] X. Xiong, C. Zhang, Y. Zhang, R. Fan, X. Qian, X.C. Dong, Fabp4-Cre-mediated Sirt6 deletion impairs adipose tissue function and metabolic homeostasis in mice, J. Endocrinol. 233 (2017) 307–314.
[16] B. Schwer, B. Schumacher, D.B. Lombard, C. Xiao, M.V. Kurtev, J. Gao, J.I. Schneider, H. Chai, R.T. Bronson, L.H. Tsai, C.X. Deng, F.W. Alt, Neural sirtuin 6 (Sirt6) ablation attenuates somatic growth and causes obesity, Proc. Natl. Acad. Sci. U. S. A. 107 (2010) 21790–21794.
[17] J. Guo, L. Dou, X. Meng, Z. Chen, W. Yang, W. Fang, C. Yang, X. Huang, W. Tang, J. Yang, J. Li, Hepatic MiR-291b-3p mediated glucose metabolism by directly targeting p65 to upregulate PTEN expression, Sci. Rep. 7 (2017) 39899.
[18] S. Zhu, F. Sun, W. Li, Y. Cao, C. Wang, Y. Wang, D. Liang, R. Zhang, S. Zhang, H. Wang, F. Cao, Apelin stimulates glucose uptake through the PI3K/Akt pathway and improves insulin resistance in 3T3-L1 adipocytes, Mol. Cell. Biochem. 353 (2011) 305–313.
[19] B. Ke, X. Ke, X. Wan, Y. Yang, Y. Huang, J. Qin, C. Hu, L. Shi, Astragalus polysaccharides attenuates TNF-alpha-induced insulin resistance via suppression of miR-721 and activation of PPAR-gamma and PI3K/AKT in 3T3-L1 adipocytes, Am. J. Transl. Res. 9 (2017) 2195–2206.
[20] P. Kong, R. Chi, L. Zhang, N. Wang, Y. Lu, Effects of paeoniflorin on tumor necrosis factor-alpha-induced insulin resistance and changes of adipokines in 3T3-L1 adipocytes, Fitoterapia 91 (2013) 44–50.
[21] D. Luna-Vital, M. Weiss, E. Gonzalez de Mejia, Anthocyanins from purple corn ameliorated tumor necrosis factor-alpha-induced inflammation and insulin resistance in 3T3-L1 adipocytes via activation of insulin signaling and enhanced GLUT4 translocation, Mol. Nutr. Food Res. 61 (2017).
[22] L.A. Salazar-Olivo, R. Mejia-Elizondo, A.J. Alonso-Castro, P. Ponce-Noyola, V. Maldonado-Lagunas, J. Melendez-Zajgla, V.M. Saavedra-Alanis, SerpinA3g participates in the antiadipogenesis and insulin-resistance induced by tumor necrosis factor-alpha in 3T3-F442A cells, Cytokine 69 (2014) 180–188.
[23] X. Meng, J. Guo, W. Fang, L. Dou, M. Li, X. Huang, S. Zhou, Y. Man, W. Tang, L. Yu, J. Li, Liver MicroRNA-291b-3p promotes hepatic lipogenesis through negative regulation of adenosine 5'-monophosphate (AMP)-activated protein kinase alpha1, J. Biol. Chem. 291 (2016) 10625–10634.
[24] R. Zhang, H. Li, Q. Guo, L. Zhang, J. Zhu, J. Ji, Sirtuin6 inhibits c-triggered inflammation through TLR4 abrogation regulated by ROS and TRPV1/CGRP, J. Cell. Biochem. 119 (2018) 9141–9153.
[25] E. Lee, D.Y. Jung, J.H. Kim, P.R. Patel, X. Hu, Y. Lee, Y. Azuma, H.-F. Wang, N. Tsitsilianos, U. Shafiq, Transient receptor potential vanilloid type-1 channel regulates diet-induced obesity, insulin resistance, and leptin resistance, FASEB J. 29 (2015) 3182–3192.
[26] Z. Xiahou, X. Wang, J. Shen, X. Zhu, F. Xu, R. Hu, D. Guo, H. Li, Y. Tian, Y. Liu, H. Liang, NMI and IFP35 serve as proinflammatory DAMPs during cellular infection and injury, Nat. Commun. 8 (2017) 950.
[27] L. Liu, X. Zhang, F. Chen, J. Hu, B. Zeng, The establishment of insulin resistance model, BIO Web of Conferences, EDP Sciences, 2017.
[28] S.P. Sah, B. Singh, S. Choudhary, A. Kumar, Animal models of insulin resistance: a review, Pharmacol. Rep. 68 (2016) 1165–1177.
[29] A.A. Romanovsky, M.C. Almeida, A. Garami, A.A. Steiner, M.H. Norman, S.F. Morrison, K. Nakamura, J.J. Burmeister, T.B. Nucci, The transient receptor potential vanilloid-1 channel in thermoregulation: a thermosensor it is not, Pharmacol. Rev. 61 (2009) 228–261.
[30] L. Negri, R. Lattanzi, E. Giannini, M. Colucci, F. Margheriti, P. Melchiorri, V. Vellani, H. Tian, M. De Felice, F. Porreca, Impaired nociception and inflammatory pain sensation in mice lacking the prokineticin receptor PKR1: focus on interaction between PKR1 and the capsaicin receptor TRPV1 in pain behavior, J. Neurosci. 26 (2006) 6716–6727.
[31] M.J. Caterina, A. Leffler, A. Malmberg, W. Martin, J. Trafton, K. Petersen-Zeitz, M. Koltzenburg, A. Basbaum, D. Julius, Impaired nociception and pain sensation in mice lacking the capsaicin receptor, science 288 (2000) 306–313.
[32] M.J. Gunthorpe, S.L. Hannan, D. Smart, J.C. Jerman, S. Arpino, G.D. Smith, S. Brough, J. Wright, J. Egerton, S.C. Lappin, Characterization of SB-705498, a potent and selective vanilloid receptor-1 (VR1/TRPV1) antagonist that inhibits the capsaicin-, acid-, and heat-mediated activation of the receptor, J. Pharmacol. Exp. Ther. 321 (2007) 1183–1192.
[33] C.E. Riera, M.O. Huising, P. Follett, M. Leblanc, J. Halloran, R. Van Andel, C.D. de Magalhaes Filho, C. Merkwirth, A. Dillin, TRPV1 pain receptors regulate longevity and metabolism by neuropeptide signaling, Cell 157 (2014) 1023–1036.
[34] Q. Han, Y.H. Kim, X. Wang, D. Liu, Z.J. Zhang, A.L. Bey, M. Lay, W. Chang, T. Berta, Y. Zhang, Y.H. Jiang, R.R. Ji, SHANK3 deficiency impairs heat hyperalgesia and TRPV1 signaling in primary sensory neurons, Neuron 92 (2016) 1279–1293.
[35] P. Bareille, R.D. Murdoch, J. Denyer, J. Bentley, K. Smart, K. Yarnall, P. Zieglmayer, R. Zieglmayer, P. Lemell, F. Horak, The effects of a TRPV1 antagonist, SB-705498, in the treatment of seasonal allergic rhinitis, Int. J. Clin. Pharmacol. Ther. 51 (2013) 576–584.